Contents lists available at SciOpen

Food Science and Human Wellness

journal homepage: https://www.sciopen.com/journal/2097-0765

China Food Publishing Co.

Covalent and non-covalent interactions between catechin and anchovy derived pentapeptides PAYCS: the differential neuroprotective effects on APP/PS1 amnesia mice

Tiantian Zhao[a,b,*], Jieqiong Chen[a], Jun Liu[c], Lijun Zhang[a], Yue Luo[b], Qingrong Huang[b], Weifeng Liu[a], Yehui Zhang[a], Jianan Zhang[d,*]

[a] Sericulture & Agri-food Research Institute Guangdong Academy of Agricultural Sciences, Key Laboratory of Functional Foods, Ministry of Agriculture and Rural affairs, Guangdong Key Laboratory of Agricultural Products Processing, Guangzhou 510610, China
[b] Department of Food Science, Rutgers University, New Brunswick 08901, United States
[c] Key Laboratory of Industrial Biotechnology, Ministry of Education, School of Biotechnology, Jiangnan University, Wuxi 214122, China
[d] National Engineering Research Center for Rice and By-Product Deep Processing, School of Food Science and Engineering, Central South University of Forestry and Technology, Changsha 410004, China

ARTICLE INFO

Article history:
Received 5 June 2024
Received in revised form 2 July 2024
Accepted 3 September 2024

Keywords:
Pentapeptide
Catechin
Covalent conjugation
Non-covalent interaction
Alzheimer's disease
Memory enhancing

ABSTRACT

Interactions between proteins/peptides and polyphenols have been widely investigated to improve their properties and functions. Previous studies have shown that covalent and non-covalent products exhibit different structural and bioactivity characteristics. The pentapeptide PAYCS (PS) was reported to be neuroprotective in amnesia mice, and catechin (CA) conjugation could improve its activity. However, different mechanisms on memory deficits alleviation between covalent and non-covalent conjugates were little investigated. In this study, the structure of PS-CA (PS and CA covalent conjugates) and PS+CA (PS and CA non-covalent complex) was characterized by using HPLC-MS/MS. Single peak for newly formed compound was identified in PS-CA and modification of tyrosine (Tyr) and cystine (Cys) was observed. In the APP/PS1 transgenic mice model experiments, behavioral tests showed that PS-CA and PS+CA could both exhibit better memory enhancing effects than that of PS. The 16S rRNA results mainly showed the alteration of gut microbiota, especially the changes in the Bacteroidota/Firmicutes ratio and significant changes in the abundance of Verrucomicrobiota. Additionally, the treatments of PS+CA and PS-CA could primarily regulate the contents of certain short chain fatty acids (SCFAs) and brain neurotransmitters, respectively. The quantitative polymerase chain reaction (qPCR) results indicated that the cholinergic system, neuronal apoptosis, and partial antioxidant pathways could be also regulated by both the treatment of PS-CA and PS+CA. Correlation analysis confirmed the relationship between the abundance of Verrucomicrobiota and other factors. The serum peptidomes results revealed that PAY contained peptides were mostly identified in PS+CA group. Especially, PS+CA showed better effects on regulating certain SCFAs and 5-hydroxytryptamine (5-HT) related neurotransmitters while PS-CA exhibited better alleviation effects on behavioral tests and neuroprotection. All these results suggested that covalent and noncovalent modification of PS with CA showed different neuroprotective effects.

1. Introduction

Alzheimer's disease (AD) is an ongoing, irreversible brain condition that impacts memory, cognition, and language abilities. Although the exact cause remains uncertain, it involves the breakdown of brain cells, disconnection from other neurons, and cell death. In advanced stages, AD leads to dementia, which significantly hampers daily life due to severe cognitive decline[1]. Notably, the increasing recognition of a two-way communication system between the brain and the gut, especially emphasizing the influence of gut microbiota in this relationship, has paved the way for exploring the molecular mechanisms behind neurological disorders[2]. This, in turn, offers new possibilities for uncovering innovative disease-alleviation approaches. Additionally, this communication involves several

* Corresponding authors.
E-mail address: fettzhao1989@163.com (T.T. Zhao); fez.jianan@foxmail.com (J.N. Zhang).
Peer review under responsibility of Beijing Academy of Food Sciences.

SciOpen Publishing services by Tsinghua University Press

http://doi.org/10.26599/FSHW.2024.9250402

pathways, including the vagus nerve, the neuroimmune system, the enteroendocrine system, neurotransmitters, branched-chain amino acids, short chain fatty acids (SCFAs) and others[3]. Therefore, apart from drug intervention, dietary approaches for the prevention of AD and improvement of AD-related symptoms are widely investigated in recent decades[4-5].

Previous studies have found that bioactive peptides derived from food protein hydrolysates exhibited positive effects on neurodegenerative diseases through the modulation of gut-brain axis[6], including the alteration of gut microbiota and its related metabolites, the brain neurotransmitters and their underlying mechanisms. Wang et al. reported that oral and intraperitoneal administration of walnut-derived pentapeptide Pro-Pro-Lys-Asn-Trp (PW5) showed alleviation effects on cognitive deficits in APPS/PS1 mice *via* the modulation of gut microbiota community and reduction of amyloid-β (Aβ) deposition[7]. Specifically, pentapeptide PAYCS (PS) exhibited modulating effects on gut microbiota-gut metabolites and brain neurotransmitters in scopolamine-induced amnesia mice, resulting in memory enhancement[8]. Unfortunately, a reduction in the bioactivity of PS was observed when subjected to simulated digestion[9]. Efforts were made to enhance its activity through interaction with catechin (CA), which exhibited inhibitory effects on digestive enzymes[10]. Nevertheless, distinct functions were discovered in covalent and noncovalent conjugation products prepared with PS and CA in our preliminary experiments.

The modification of proteins and peptides including physical, chemical, bioengineering and other new technologies[11]. Among them, chemical modifications were widely investigated due to the structural modifications and synergistic effects for their properties and bioactivities. Accordingly, the interactions between peptides/proteins and polyphenols could be divided into 2 categories: covalent and non-covalent which would lead to the changes in structures, properties, functions, and bioactivities[12]. The main forces involved in non-covalent binding are hydrogen bonding and hydrophobic interactions. Meng et al.[13] found that gallic acid (GA), CA and epigallocatechin gallate (EGCG) were bound with whey protein isolate (WPI) through non-covalent interactions to form complexes, which led to a partially unfolded protein structure and higher surface hydrophobicity and enhanced solubility, foaming and emulsifying capacities of WPI. Compared to covalent bonds, the non-covalent interactions are relatively weak and unstable. Furthermore, phenolic compounds, such as CA with phenolic hydroxyl groups in food matrices, can form phenoxy radicals through oxidation[14] and covalently interact with polypeptides having nucleophilic reactive groups, thus affecting their bioactive and digestive properties. Wu et al.[15] found that the emulsifying and antioxidant properties of soy protein hydrolysates were effectively enhanced by EGCG covalent modification. To improve the anti-digestive properties of PS, we previously prepared covalent and non-covalent conjugates between PS and CA. Additionally, the memory improvement effects of CA and PS were reported in our previous investigations, the results showed that covalent interaction of PS with CA could enhance the brain function enhancement effects of PS in scopolamine induced amnesia mice model[10]. Notably, the researchers were focusing on the interactions between protein and polyphenols or the emulsification effects of these conjugates. However, the specific structures of covalent and non-covalent peptide-polyphenol conjugates and their differential effects on neuroprotective functions remain unknown.

In this study, we aim to investigate the structural and brain enhancement effects of covalent and non-covalent interaction products of PS and CA. Furthermore, APP/PS1 transgenic C57BL/6J mice were employed in this study to explore the differential mechanisms of sample on potential memory alleviation effects. These results were aimed to provide a comprehensive understanding of the differential memory-enhancing effects between covalent and non-covalent peptide-polyphenol compounds.

2. Materials and methods

2.1 Materials and chemicals

PS was chemically synthesized by GL Biochem Ltd. (Shanghai, China) and stored at −20 ℃ until use. The purity of the peptide was greater than 95%. CA, acetic acid, propanoic acid, butanoic acid, isobutyric acid, valeric acid, isovaleric acid, hexanoic acid, isohexanoic acid and 2-ethylbutyric acid, 5-hydroxyindole acetic acid (5-HIAA), serotonin (5-HT), serine (Ser), acetylcholine (Ach), dopamine (Da), dihydroxyphenylacetic acid (Dopac), cysteine (Cys), kynurenine (kyn), gamma-aminobutyric acid (GABA), glutathione (GSH), glutamine (Gln), glutamate (Glu), homovanillic acid (HVA), Levodopa (LDOPA), norepinephrine (NE), lysine (Lys), phenylalanine (Phe), spermine (Spm) and spermidine (Spd) were purchased from Sigma Chemical Co., Ltd. (St. Louis, MO, USA). Reagents used for high-performance liquid chromatography tandem mass spectrometry (HPLC-MS/MS) analysis were of HPLC grade. All other reagents used were of analytical grade.

2.2 Preparation of covalent and non-covalent interaction products of PS and CA

The covalent conjugates of CA and PS were prepared according to the method of our previous research with some modifications[10]. Briefly, a certain quality of CA was dispersed in an appropriate amount of methanol and then diluted with distilled water to a final volume of 200 mL. The pH of the CA solution was adjusted to 9.0 with 0.1 mol/L NaOH and stirred for 12 h to ensure complete dispersion. Then, PS was dissolved to a final volume of 200 mL with distilled water. The pH was adjusted to 9.0 with 0.1 mol/L NaOH. The PS solution was then mixed with CA solutions at a ratio of 5:1 and continuously stirred at room temperature for another 24 h to ensure a complete reaction between PS and CA. Afterward, the samples were dialyzed against several water changes to eliminate the free unbound CA, followed by lyophilization to acquire covalent PS-CA complexes. This sample is referred to as “PS-CA”. Based on the procedure, non-covalent PS and CA mixtures (ratio of 5:1) were prepared at pH 7.0 without oxygen and referred to as “PS+CA”.

2.3 Identification and characterization of samples

Chromatographic analysis of the digested and control samples was carried out using a HPLC system with an automatic injector and a diode-array detector (DAD) (Agilent 1200 Series, Snoqualmie, WA, USA). Separation was achieved on a ZORBAX Eclipse XDB-C18 column (4.6 mm × 250 mm, 5 μm) at a flow rate of 1 mL/min, 25 °C. A total of 5 mL of samples (1 mg polypeptides per mL) and control

samples (1 mg protein per mL) were injected into the column after filtration through 0.22 μm membranes.

2.4 Nano LC-MS/MS analysis of PS-CA conjugates

The CA-PS conjugates were further identified by HPLC-DAD-MS/MS. Nanocolumn 150 μm × 15 cm in-house made column packed with a reversed-phase ReproSil-Pur C18-AQ resin (1.9 μm, 100 Å, Dr. Maisch GmbH, Germany); Loaded sample volume: 5 μL; Mobile phase: A: 0.1% formic acid in water; B: 0.1% formic acid in water (20%)-acetonitrile (80%). Total flow rate: 600 nL/min; LC linear gradient: from 6% to 9% B for 5 min, from 9% to 14% B for 15 min, from 14% to 30% B for 30 min, from 30% to 40% B for 8 min and from 40% to 95% B for 2 min. Operation parameters were as follows: spray voltage: 2.2 kV; capillary temperature: 270 °C; MS resolution: 70 000 at *m*/*z* 400; MS precursor *m*/*z* range: 400.0–1 200.0. MS/MS parameters: product ion scan range: start from *m*/*z* 50; activation type: higher-energy collisional dissociation (HCD); normalized coll. Energy: 28.0 eV; activation time: 60.000 ms; data-dependent MS/MS: up to the top 20 most intense peptide ions from the preview scan in the Orbitrap.

2.5. Animal experiments

2.5.1 Ethics statement

All the procedures and experimental design involved in this study were performed according to the Guidelines of Animal Ethical and Welfare Committee (AEWC). The experimental protocols were reviewed and approved by Guangzhou Yongnuo Medical Laboratory Animal Center Ethics Committee and the approval number was IACUC-AEWC-F2204024.

2.5.2 Animals

APP/PS1 transgenic male mice (5−8 weeks, n = 32) and C57BL/6J male mice (8 weeks, n = 8) weighing 18.0−22.0 g were chosen and provided by the Changzhou Cavens Laboratory Animals Co., Ltd. (Changzhou, China), certificate No. SCXK (Su) 2021-0013. During this study, mice were fed autoclaved chow and water *ad libitum* under a 12 h light/12 h dark cycle and a constant temperature of 21−22 °C and humidity of (55 ± 5)%.

2.5.3 Treatments

The mice were randomly allocated into 5 groups, each comprising 8 individuals. The treatment regimens were as follows: Based on prior researches[8-10], the groups designated as PS+CA, PS-CA, and PS were administered PS+CA, PS-CA, and PS, respectively, each in an aqueous solution at a concentration of 0.2 g/kg body weight (BW) daily *via* intragastric administration for 8 weeks. The control group, consisting of C57BL/6J mice, and the model group, comprising APP/PS1 mice, received an equivalent volume of distilled water through the same route. All groups were subsequently subjected to the Morris water maze (MWM) test for the assessment of cognitive functions.

2.5.4 MWM tests

This spatial navigation test was designed to measure the acquisition of learning and memory capabilities in mice. It involved observing and recording the routes taken by the mice to find and climb onto a platform, as well as the time required to do so, known as the escape latency. Water Maze System (Guangzhou Bite Biological Co., Ltd., Product Code B001) was applied in this study.

According to previous study[9], 5 days prior to euthanasia, the training phase of the experiment was conducted over 4 consecutive days, with 4 trials per day. During training, mice were released into the pool facing the wall from 4 different entry points. The time taken by each mouse to locate and stand on the submerged platform was recorded in seconds as the latency period. Once a mouse found the platform, it was allowed to stand on it for 15 s. If a mouse failed to find the platform within 120 s after entering the water, it was gently guided onto the platform and allowed to remain there for 15 s before the next trial. Each mouse was released into the pool from each of the 4 entry points once per training session, with a 30-s interval between trials. Following the 4 days of training, the official experiment commenced on the 5th day. The platform was removed. Subsequently, the test mice were introduced into the water in a clockwise direction, starting from the first quadrant. The number of times each mouse crossed the original platform location within a 2-min period was measured, along with the time and distance spent in each quadrant where the platform was previously located. Additionally, the swimming distance and speed of the mice were recorded. These measures were used to assess the mice's memory retention and retrieval capabilities. Emphasis was placed on recording data related to the third quadrant.

2.5.5 16S rRNA gene sequencing and analysis

Fecal samples from each mouse were meticulously collected, and microbial DNA was extracted using the E.Z.N.A. Soil DNA kit (Qiagen, USA). Subsequently, the 16S rRNA gene sequencing was performed, following the methodologies described by Zhao et al.[10], using an ABI GeneAmp 9700 PCR thermocycler (Applied Biosystems, CA, USA).

2.5.6 SCFAs analysis

In the sample processing protocol, 25 mg of fecal sample was placed in a 2 mL grinding tube with 500 μL of 0.5% phosphoric acid solution. This was followed by a freeze-grinding process at 50 Hz for 3 min, repeated twice, and ultrasonication for 10 min. After centrifugation at 4 °C and 13 000 × *g* for 15 min, the supernatant was collected into a 1.5 mL centrifuge tube. Extraction was performed by adding 0.2 mL of *n*-butanol containing 10 μg/mL of 2-ethylbutyric acid as an internal standard. The mixture was then vortexed for 10 s, ultrasonicated at low temperature for 10 min, and centrifuged again at 4 °C and 13 000 × *g* for 5 min. The final supernatant was transferred to a sample vial for subsequent instrumental analysis.

The analytical instrument used in this experiment was the Agilent 8890B-5977B GC/MSD system, provided by Agilent Technologies Inc. (CA, USA). Chromatographic conditions were set using an HP FFAP capillary column (30 m × 0.25 mm, 0.25 μm, Agilent J&W

Scientific, Folsom, CA, USA). The carrier gas was high-purity helium (purity ≥ 99.999%), with a flow rate of 1.0 mL/min. The temperature of the injection port was maintained at 180 ℃. The injection volume was 1 μL, using a split mode with a split ratio of 10:1, and a solvent delay of 2.5 min. The temperature program started at an initial column temperature of 80 ℃, then increased at a rate of 20 ℃/min to 120 ℃, followed by a ramp of 5 ℃/min to 160 ℃, and finally held at 220 ℃ for 3 min. Mass spectrometric conditions were set with an electron ionization (EI) source at a temperature of 230 ℃, quadrupole temperature at 150 ℃, and transfer line temperature at 230 ℃. The electron energy was set at 70 eV. The scanning mode was selective ion monitoring (SIM). The MassHunter Quantitative Software (Agilent Technologies, USA, Version: v10.0.707.0) was employed with default parameters for the automatic identification and integration of ion fragments of target SCFAs, supplemented by manual verification. The detection concentrations of each sample were calculated using standard curves, which were then used to determine the actual content of SCFA in the samples.

2.5.7 Analysis of neurotransmitters in mice brain

The brain tissues were harvested through a meticulous process that began with humane euthanasia, followed by careful cranial dissection to expose the skull. The skull was then gently opened to avoid brain tissue damage, allowing for the delicate removal of the brain. Then the neurotransmitters were then extracted and detected according to previous methods[10]. The UHPLC separation was carried out using an ExionLC System, equipped with a Waters ACQUITY UPLC HSS T3 (100 mm × 2.1 mm, 1.8 μm). The mobile phase A was 0.1% formic acid and 1 mmol/L ammonium acetate in water, and the mobile phase B was acetonitrile. The column temperature was set at 40 ℃. The auto-sampler temperature was set at 4 ℃ and the injection volume was 1 μL. AB Sciex QTrap 6500+ mass spectrometer was applied for assay development. Typical ion source parameters were: IonSpray voltage: +5 000 V, curtain gas: 35 psi, temperature: 400 ℃, ion source gas 1: 60 psi, ion source gas 2: 60 psi. Skyline software was employed for MRM data processing.

2.5.8 Analysis of related pathway factors in mice brain by quantitative polymerase chain reaction (qPCR)

qPCR was applied to quantify the transcription gene levels of brain function related pathway factors. Briefly, total RNA of tissues was extracted by using TRIzol reagent according to manufacturer's protocol. The cDNA was synthesized by reverse transcription reaction, and then amplified by real-time fluorescence quantitative PCR and thermal cycler. qPCR was measured by SYBR Premix Ex *Taq* on gene amplifiers. The primer information was provided in Table S1. The mRNA expression was calculated as a fold change of gene expression.

2.5.9 Peptides analysis in serum

After behavioral tests, all mice were sacrificed. Subsequently, blood samples were collected in heparinized tubes through enucleation. These samples were centrifuged at 3 000 r/min for 15 min to separate the plasma, which was subsequently stored at −80 °C until further analysis.

In the peptide extraction process, 100 μL of the sample was placed into a 10 kDa ultrafiltration tube and mixed with 400 μL of 25 mmol/L NH_4HCO_3-10% ACN solution, followed by vertexing and incubation at room temperature for 1 h. This was succeeded by centrifugation at 12 000 × *g* for 10 min at 4 °C, a process repeated after adding 200 μL of water. The resultant peptides were vacuum-dried and then desalted using a self-packed column, followed by a final vacuum drying at 45 °C for storage.

In the LC-MS/MS experiment, a 150 μm i.d. × 150 mm Acclaim PepMap RPLC C_{18} column was used with mobile phases of 0.1% formic acid (A) and 0.1% formic acid in 80% ACN (B), at a flow rate of 600 nL/min over a 120-min gradient. The MS analysis involved a primary resolution of 70 000 with an AGC target of 3×10^6 and a scan range of *m/z* 350−1 500, and a secondary resolution of 75 000 with an AGC target of 1×10^5 and a top *n* of 20. Peptide sequencing was performed using Peaks Studio 8.5 for *de novo* analysis, considering carbamidomethyl (C) as a fixed modification and oxidation as a variable modification, with a peptide mass tolerance of 20×10^{-6} and a fragment mass tolerance of 0.02 Da.

2.6 Statistical analysis

Statistical analysis and correlation analysis were conducted using GraphPad Prism 10.0, with data presented as mean ± standard deviation. One-way analysis of variance (ANOVA) followed by Duncan's multiple range test was utilized to identify significant differences between group means ($P < 0.05$). Spearman's correlation coefficients were employed for the correlation analysis among different groups. The 16S rRNA gene sequences of the gut microbiota and their correlation relationships were examined using the online platform http://www.i-sanger.com.

3. Results

3.1 Structural identification of covalent and non-covalent catechin-pentapeptide conjugates

To identify the formation of covalent and non-covalent complexes, RP-HPLC was employed. The chromatographic spectra of the samples with covalent and non-covalent treatment are shown in Figs. 1A-D. Complex identification was conducted by comparing the retention times of peaks in the sample with CA and PS, exhibiting retention times of 9.0 min for CA and 6.4 min for PS. However, the peaks of the PS+CA were detected at both 6.4 and 9.0 min, indicating that the complete sequence of the native PS and CA could be detected in the complexes of PS+CA. While the conjugation PS-CA only showed a peak at a retention time of 7.3 min (affecting the peptide hydrophobicity and thus prolonging the retention time)[16]. This also indicated that the conjugates were produced, and the covalent conjugation occurred between CA and PS was consistent with the previous report on wheat gliadin[17]. It could be assumed that during the covalent interactions, new substances were produced in PS-CA. The structure would be further carefully investigated.

LC-MS/MS was used to further confirm covalent bonding and evaluate the molecular weight change of conjugates. The results were documented in Fig. 1E. The main peak with a molecular weight of 867.29 Da was found in the PS-CA, corresponding to PS (540.21 Da),

consistent with the observation found by Zhao et al.[9]. The increase of molecular mass of PS after conjugation with CA (increase by 327 Da) confirmed the successful covalent attachment of the CA molecule to PS. This was consistent with the apparent increase in the molecular weight of α-lactalbumin after conjugation with CA[18].

The oxidation of phenol rings to quinone derivatives, which are extremely reactive with nucleophilic residues (such as amino and sulfhydryl groups) on proteins or peptides by Michael addition[19-20]. CA could be turned into *o*-quinones when driven by pH and oxygen and reacted with Cys or tyrosine (Tyr) or Ser of PS to produce structural changes. Fig. 1F shows that PS covalently interacted with CA to produce dehydration condensation grafting (+270) at the Tyr position with the *o*-quinone formed from CA, while at Cys, an alkylation modification (+57) was produced due to the reaction

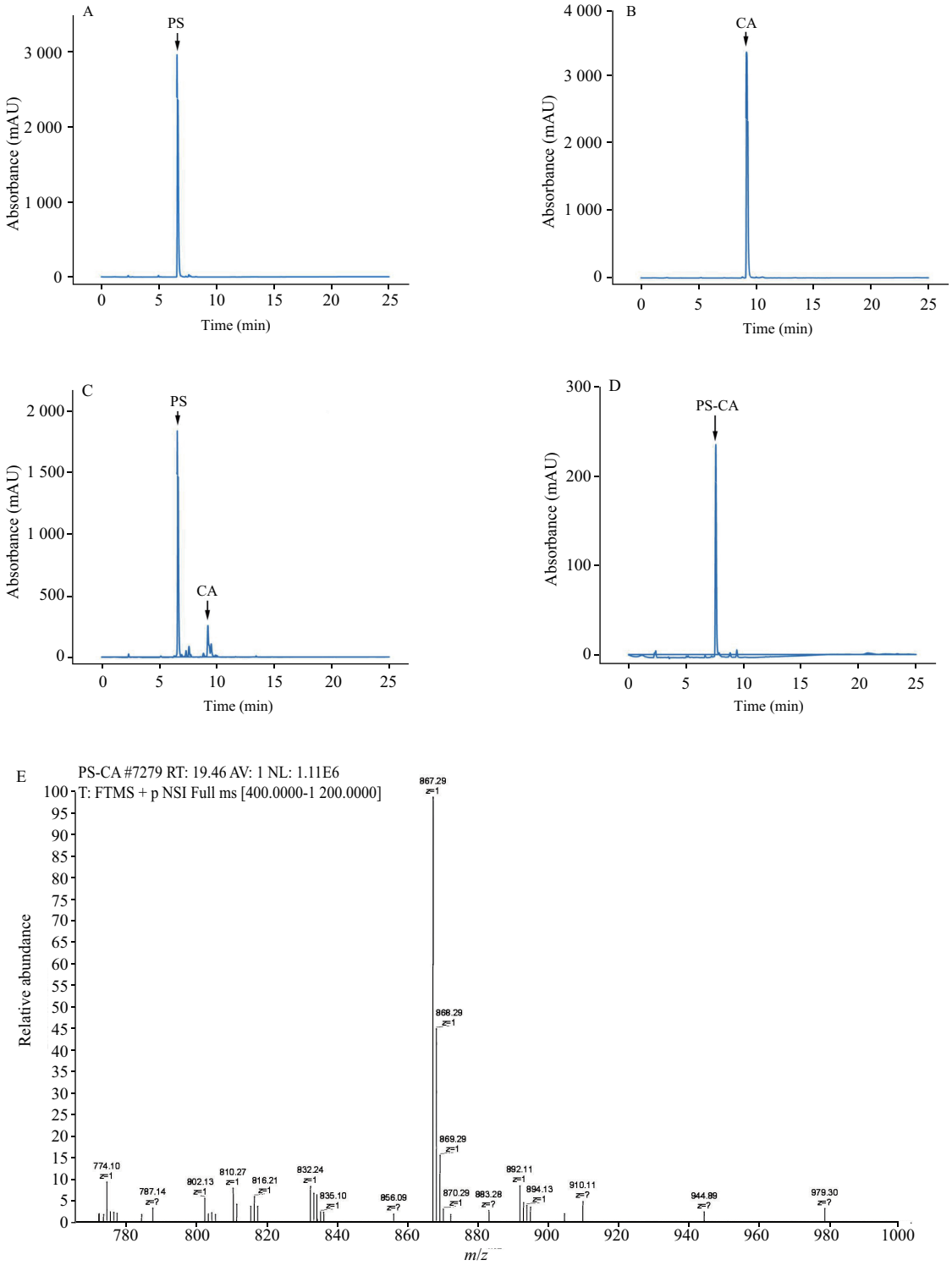

Fig. 1 RP-HPLC chromatograms of (A) PS , (B) CA, (C) PS+CA and (D) PS-CA and (E) MS and (F) MS/MS spectra of PS-CA.

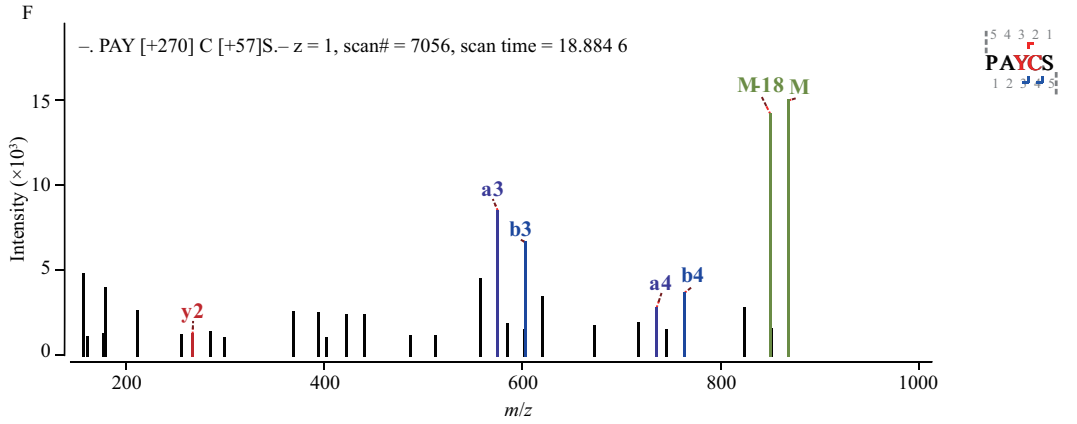

Fig. 1 (*Continued*)

environment. Covalent conjugation between CA and PS was further proved with LC-MS/MS and the *m/z* of PS-CA formed in this study was speculated to be 867.29 Da (Fig. 1E). We would explore its specific structure with purification, enrichment, and nuclear magnetic resonance analysis.

3.2 Effects of samples on memory impairments of APP/PS1 amnesia mice

The APP/PS1 transgenic mouse model is widely utilized in the investigation of AD pathogenesis, representing one of the most prevalent animal models in this research area[21]. In this study, APP/PS1 transgenic mice exhibiting amnesic symptoms received administrations of PS-CA, PS+CA, and PS, while wild-type mice served as controls. Behavioral test data collected during the training phase are presented in Figs. 2A-D. Fig. 2A reveals that, during training, all groups exhibited a downward trend in escape latency, suggesting that training facilitated the recollection of mice for the target platform's location. On the 4th day of training, the APP/PS1 model group demonstrated significantly prolonged escape latency compared to the control group ($P < 0.01$). The administration of the test compounds markedly ameliorated this effect in the order of PS-CA, PS+CA, and PS. Trends in swimming distance paralleled those observed for escape latency. The number of crossing times refers to the instances when mice traversed the target platform's location. As depicted in Fig. 2C, on the fourth day, crossing times in the model group were substantially reduced compared to the control group ($P < 0.05$). Treatment with PS-CA and PS notably increased crossing times ($P < 0.05$). Based on the average speed results, which showed no significant differences, we inferred that all mice maintained comparable physiological conditions.

Figs. 2E-H presented the behavioral test outcomes from the testing phase. The data indicated that the APP/PS1 model group experienced significantly longer escape latencies and fewer platform

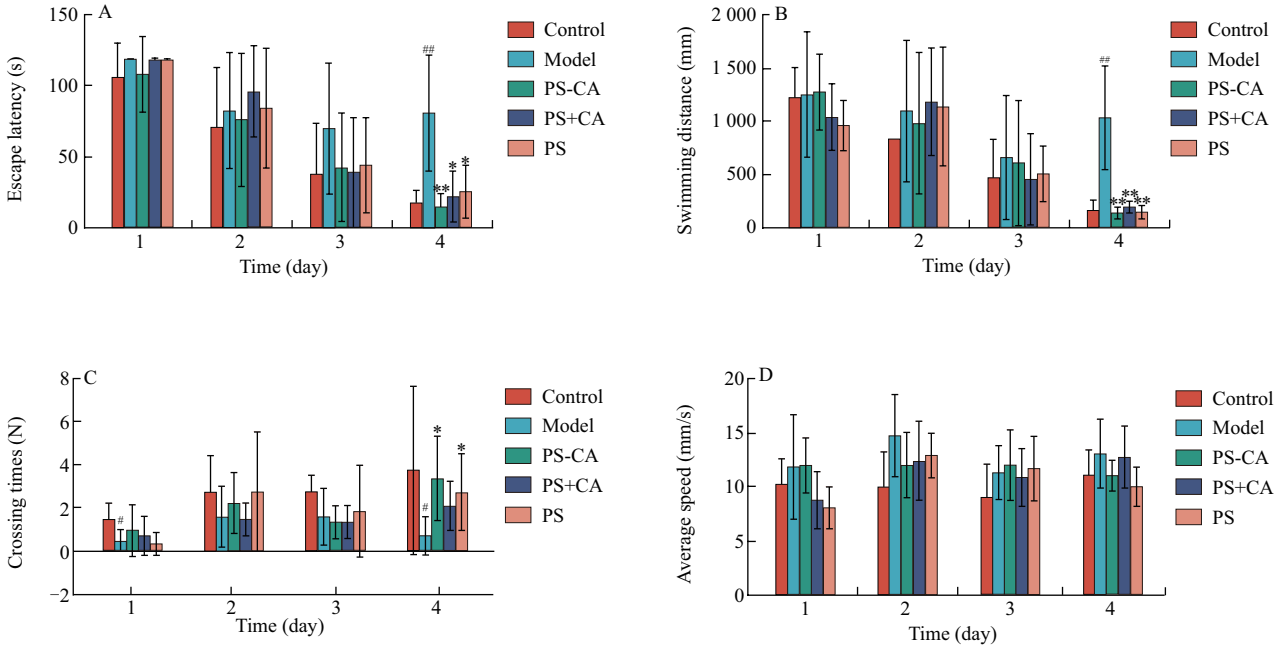

Fig. 2 Effects of samples on the behavioral tests of APP/PS1 mice. (A) Escape latency, (B) swimming distance, (C) number of crossing times of the target platform, (D) average speed, (E) escape latency, (F) swimming distance, (G) number of crossing times of the target platform, and (H) average speed during the testing part were determined. $^{\#}P < 0.05$, $^{\#\#}P < 0.01$ *vs.* control group; $^{*}P < 0.05$, $^{**}P < 0.01$ *vs.* model group.

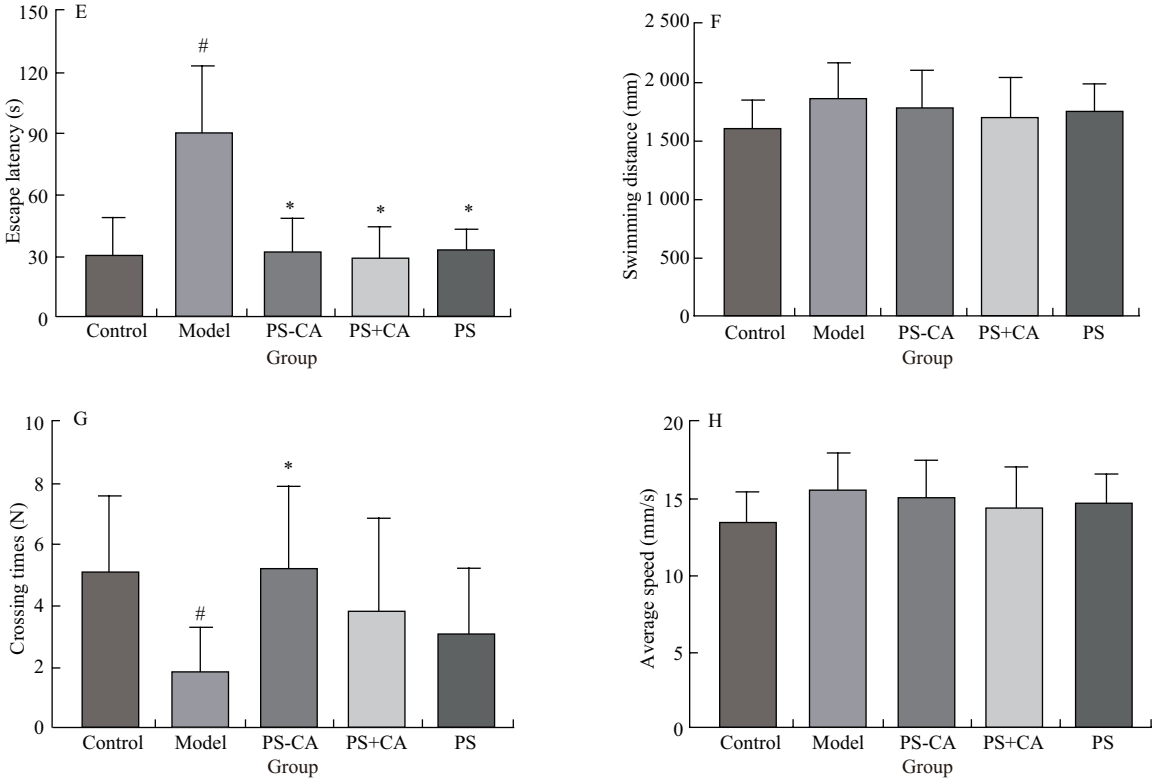

Fig. 2 (*Continued*)

crossings compared to the control group. The administration of the therapeutic compounds substantially reduced escape latencies and increased platform crossings, signifying an effective mitigation of memory deficits in the APP/PS1 mouse model. Notably, PS-CA demonstrated superior efficacy among the treatments assessed.

3.3 Effects of samples on gut microbiota composition of APP/PS1 amnesia mice

Emerging studies increasingly substantiate the notion that equilibrium within the gut microbiota is intricately connected to cerebral function, thereby underpinning the microbiota-gut-brain axis hypothesis[22]. In this investigation, we characterized the gut microbiota composition across different experimental cohorts. Fig. 3A illustrated that, while no significant differences were detected among the treatment groups, variation in the Shannon diversity index at the operational taxonomic unit (OTU) level was observed, which corresponded to differences in species composition at the OTU level as depicted in Fig. 3B. Community barplot analysis, as shown in Fig. 3C, indicated an upregulation in the relative abundance of Proteobacteria, Actinobacteriota, Campilobacterota, and Verrucomicrobiota in the APP/PS1 mice, whereas Bacteroidota, Patescibacteria, and Desulfobacterota were found to be downregulated. Treatment with the experimental compounds resulted in a reduction of Firmicutes and Verrucomicrobiota (Fig. 3E) and an elevation in Bacteroidota (Fig. 3F) abundance compared to the model group. Specifically, PS-CA treatment was associated with a decrease in Proteobacteria, Desulfobacterota, Actinobacteriota, and Verrucomicrobiota abundance, and an increase in Patescibacteria and Campilobacterota. The PS+CA treatment decreased the levels of Proteobacteria, Patescibacteria, Desulfobacterota, Actinobacteriota, and Verrucomicrobiota, but increased Campilobacterota. Furthermore, PS treatment increased the abundance of Proteobacteria, Patescibacteria, and Desulfobacterota while reducing Campilobacterota levels (Table S2).

We further explored the variances in microbial community structures across distinct treatment cohorts. The principal component analysis (PCA), depicted in Fig. 3D, showed clear separations among bacterial communities of different treatment groups, apart from those receiving PS-CA and PS. Notably, the disparity in microbial composition between the control and the model groups was more pronounced than between the treatment and control groups, indicating that the interventions may exert a beneficial regulatory effect on the gut microbiota of the dementia mouse model. Furthermore, as presented in Figs. 3G and H, the Verrucomicrobiota abundance was significantly elevated in the APP/PS1 group ($P < 0.01$). However, the application of the various treatments markedly reduced its abundance ($P < 0.01$ for PS+CA group and $P < 0.05$ for PS-CA and PS groups). These findings suggested that Verrucomicrobiota might play a pivotal role in the pathophysiology studied and warrants further investigation.

3.4 Effects of samples on SCFA composition of APP/PS1 amnesia mice

SCFA, already known for helping with energy and gut health, might also influence the brain. Studies suggested an unbalanced gut can relate to brain-related conditions like depression and AD[23]. In this investigation, we quantified the levels of SCFAs in various groups (Fig. 4). Of the 8 SCFAs analyzed, acetic acid, propanoic acid, isobutyric acid, butanoic acid, isovaleric acid, valeric acid, and hexanoic acid were found to be significantly reduced in the APP/PS1

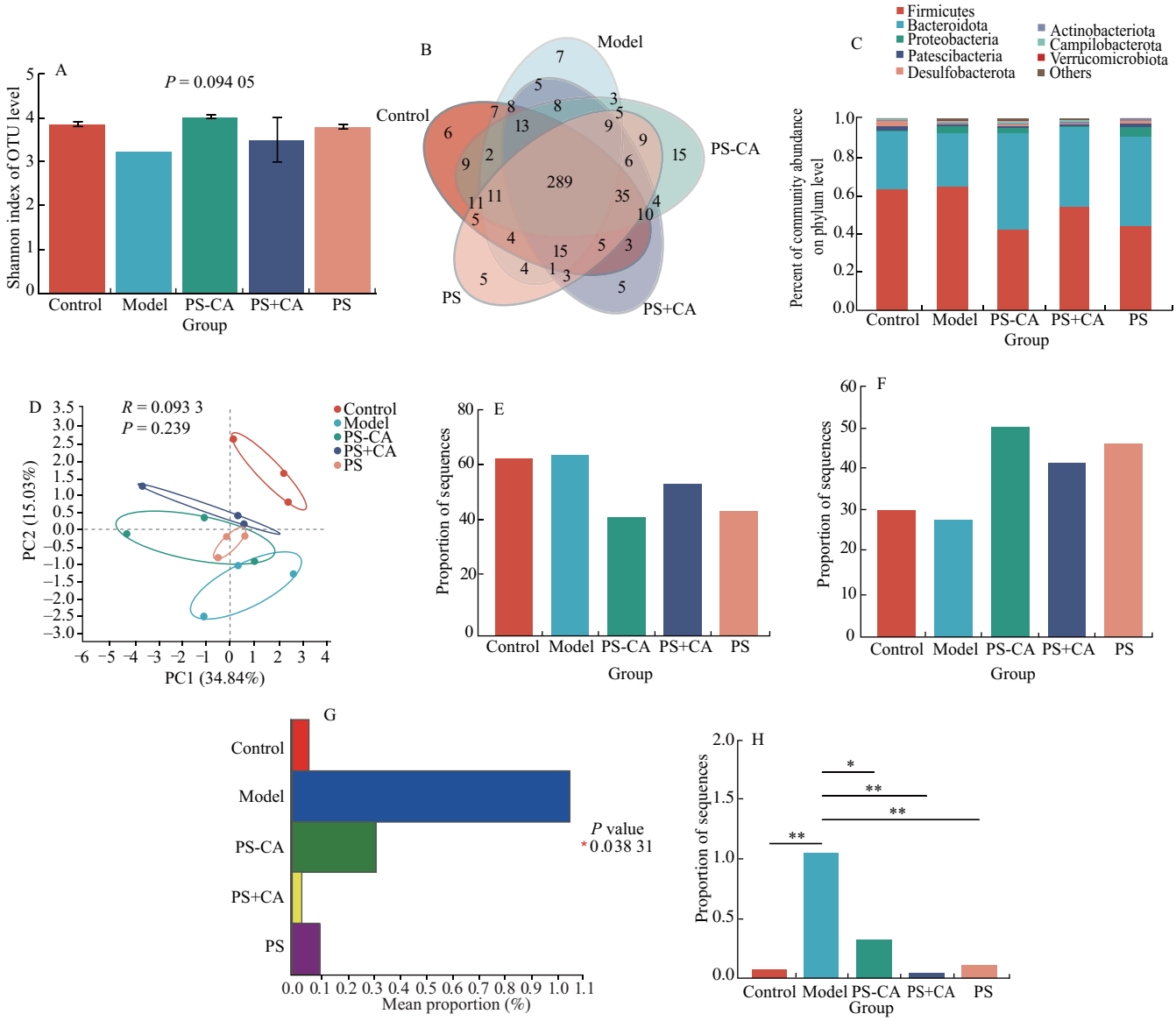

Fig. 3 Effects of samples on gut microbiota of APP/PS1. (A) Shannon index of α diversity on the OTU level, (B) Venn diagram of species composition on the OTU level, (C) community barplot analysis on the phylum level, and (D) the PCA level on phylum level, single species difference analysis bar chart for (E) Firmicutes and (F) Bacteroidota as well as (G-H) Verrucomicrobiota were presented. * and ** represent $P < 0.05$ and $P < 0.01$, respectively.

mice compared to the control group, apart from isohexanoic acid. Treatment with PS+CA effectively restored the levels of all 8 SCFAs. In contrast, PS-CA treatment only elevated the levels of acetic acid and propanoic acid. Moreover, PS administration did not significantly affect the levels of butanoic acid and valeric acid.

3.5 Effects of samples on brain neurotransmitters of APP/PS1 amnesia mice

Investigations into the gut microbiome have elucidated its associations with neuro-communication, stress response, and neuropsychiatric disorders, such as autism, depression, and schizophrenia. These findings prompt further inquiry into the role of gut bacteria in modulating critical neurotransmitters[24]. In the current study, twenty neurotransmitters were quantified in the murine brain. As depicted in Fig. 5, the levels of 5-HT, Ser, DOPAC, GABA, GSH, Gln, HVA, *L*-DOPA, Spd, and Spm were notably diminished in the APP/PS1 model group relative to the control. Treatment with PS-CA significantly augmented the concentrations of Cys, GABA, GSH, Gln, and Spd (for GSH, $P < 0.01$ and for others, $P < 0.05$), while reducing Glu content in the brain ($P < 0.05$). Conversely, PS+CA treatment markedly elevated the levels of 5-HT ($P < 0.05$), Kyn ($P < 0.05$), and Spm ($P < 0.01$). Administration of PS solely increased the Phe concentration significantly ($P < 0.05$).

3.6 Effects of samples on neuro-related pathway factors of APP/PS1 amnesia mice

Numerous pathways are known to modulate brain functions, encompassing mechanisms such as oxidative stress, inflammatory

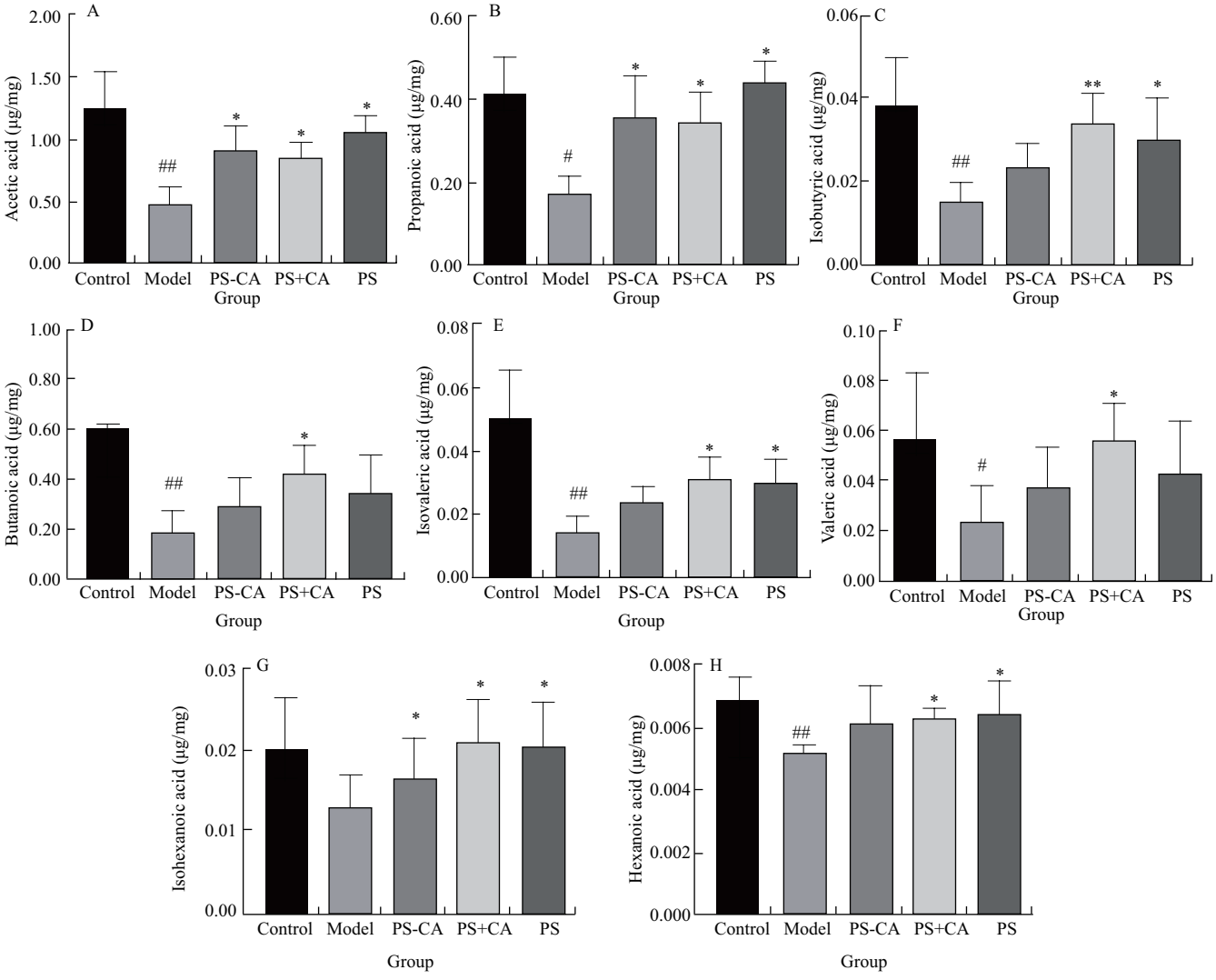

Fig. 4 Effects of samples on short-chain fatty acids (SCFAs) in the gut of APP/PS1 mice, (A) acetic acid, (B) propanoic acid, (C) isobutyric acid, (D) butanoic acid, (E) isovaleric acid, (F) valeric acid, (G) isohexanoic acid and (H) hexanoic acid. $^{\#}P < 0.05$, $^{\#\#}P < 0.01$ *vs.* control group; $^{*}P < 0.05$, $^{**}P < 0.01$ *vs*. model group.

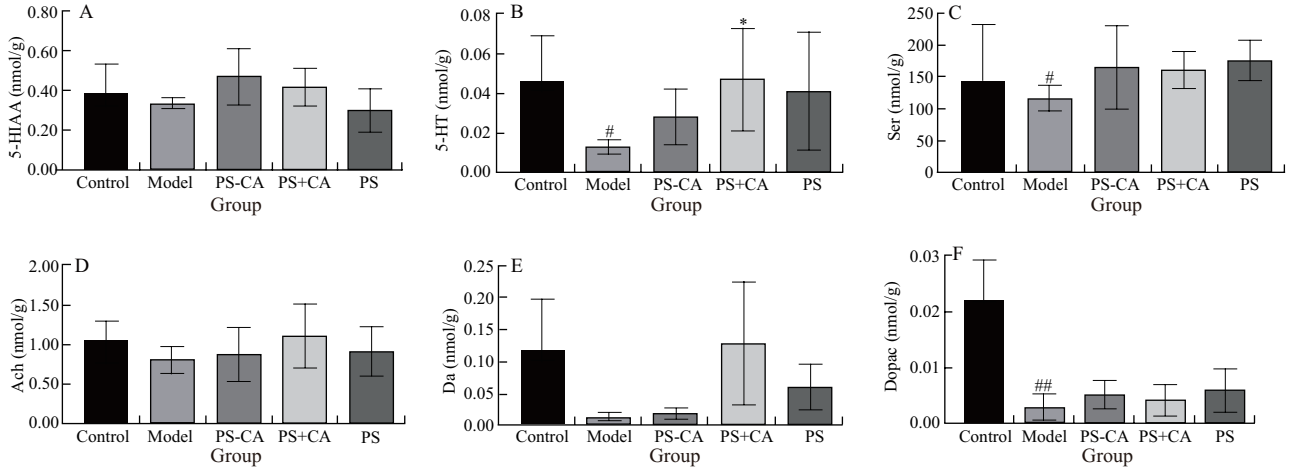

Fig. 5 Effects of samples on brain neurotransmitters in APP/PS1 mice. (A) 5-HIAA, (B) 5-HT, (C) Ser, (D) Ach, (E) Da, (F) Dopac, (G) Cys, (H) Kyn, (I) GABA, (J) GSH, (K) Gln, (L) Glu, (M) HVA, (N) LDOPA, (O) NE, (P) Lys, (Q) Phe, (R) Spd, (S) Spm, (T) Trp and (U) VMA. Only neurotransmitters with significant differences among groups are shown. $^{\#}P < 0.05$, $^{\#\#}P < 0.01$ *vs*. control group; $^{*}P < 0.05$, $^{**}P < 0.01$ *vs*. model group.

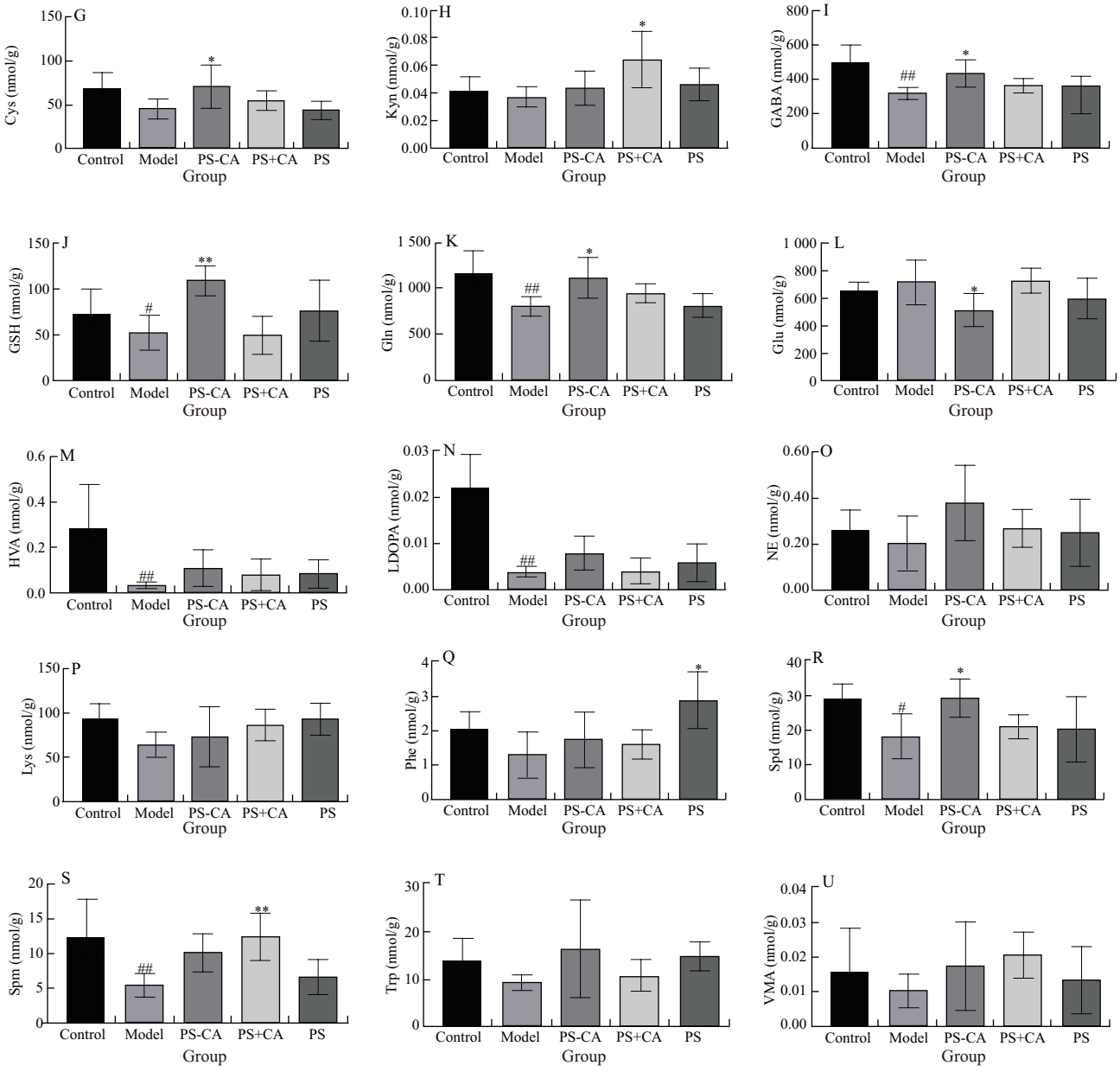

Fig. 5 (*Continued*)

responses, amyloid precursor protein (APP) metabolism, neuronal apoptosis, and various other molecular cascades[25-28]. Fig. 6 illustrates a marked increase in *APP* expression in the APP/PS1 mouse model, confirming the validity of model for studying amnesia. However, treatment with the experimental compounds did not significantly affect *APP* expression or the levels of beta-secretase 1 (*BACE1*). In the cholinergic system, the expression levels of acetylcholinesterase (*AChE*) and alpha-7 nicotinic acetylcholine receptor (*AChR-α7*) were reduced in the model group compared to the control, but these differences were not statistically significant ($P > 0.05$). Notably, PS-CA and PS+CA treatments significantly upregulated *AChE* and *AChR-α7* expression ($P < 0.05$), a change not observed with PS treatment. Regarding oxidative stress markers nuclear factor erythroid 2-related factor 2 (*Nrf2*) and *Keap1*, and pro-inflammatory cytokines interleukin 1 beta (*IL-1β*) and tumor necrosis factor alpha (*TNF-α*), no significant alterations were detected across treatment groups ($P > 0.05$). Interestingly, PS-CA and PS+CA treatments significantly increased the expression of heme oxygenase-1 (*HO-1*), which was decreased in the APP/PS1 model ($P < 0.05$). In the neuronal apoptosis pathway, the expression levels of B-cell lymphoma 2 (*Bcl-2*) and *Bcl-2*-associated X protein (*Bax*) showed no significant differences ($P > 0.05$); however, the *Bax/Bcl-2* ratio was significantly elevated in the APP/PS1 model ($P < 0.01$). The treatments with PS-CA and PS significantly lowered this ratio ($P < 0.01$ for PS-CA and $P < 0.05$ for PS), suggesting a potential mitigating effect on neuronal apoptosis.

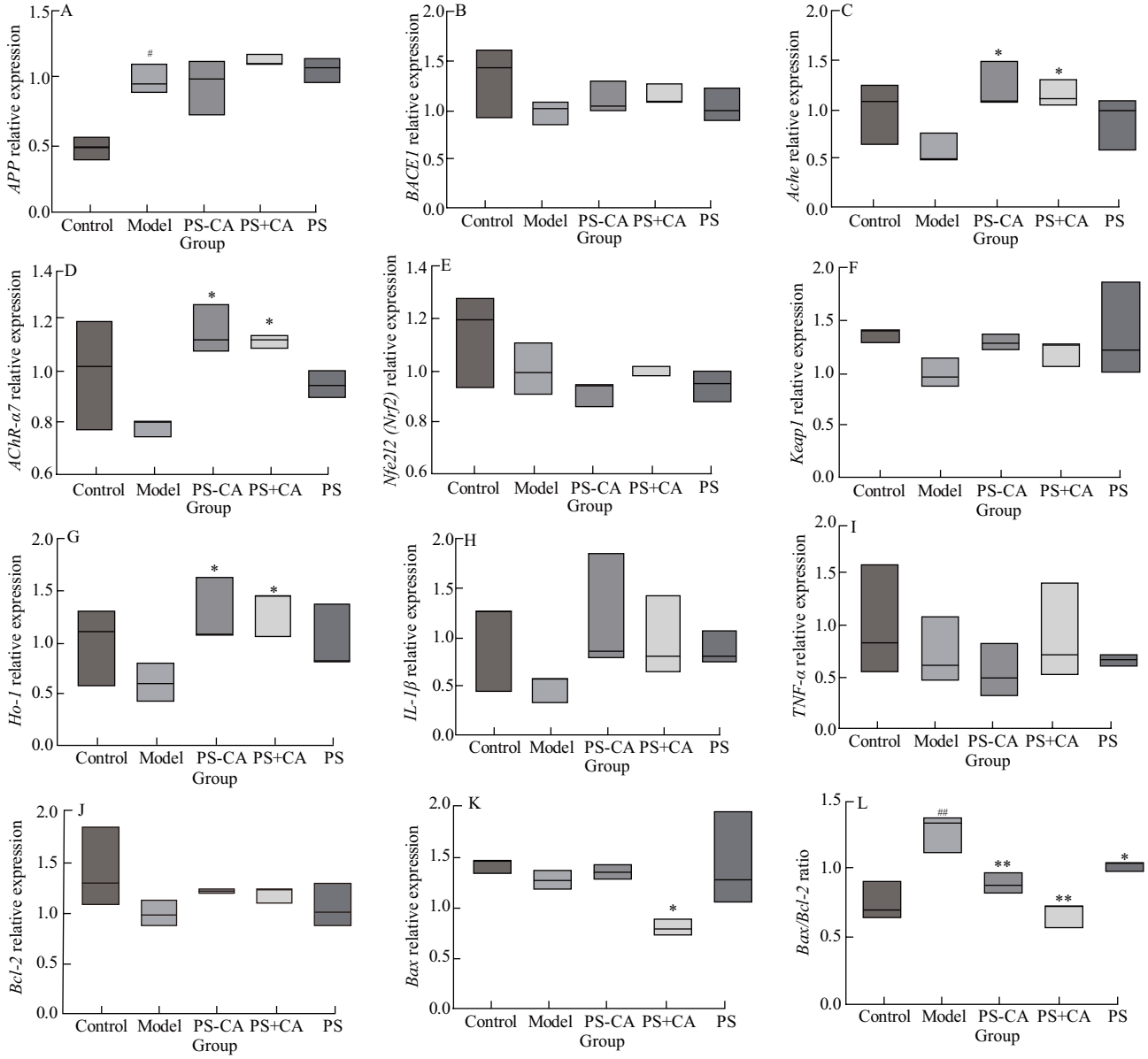

Fig. 6 Effects of samples on the mRNAexpression levels of neuro-related pathway factors in APP/PS1 mice. (A) APP, (B) BACE1, (C) AChE, (D) AChR-α7, (E) Nrf2, (F) Keap1, (G) Ho-1, (H) IL-1β, (I)TNF-α, (J) Bcl-2, (K) Bax, and (L) Bax/Bcl-2 ratio. Expression levels were normalized to the control group. Data are presented as mean ± SD (n= 8). $^{\#}P < 0.05$, $^{\#\#}P < 0.01$ *vs.* control group; $^{*}P < 0.05$, $^{**}P < 0.01$ *vs*. model group.

3.7 Correlation analysis

Numerous studies have elucidated novel microbial and metabolic frameworks that advance our understanding of the microbiota-gut-brain axis. These frameworks suggest that the regulation of gut microbiota may influence the levels of SCFAs, brain neurotransmitters, and factors associated with neuro-related pathways[29-31]. Hence, conducting a correlation analysis between various parameters is crucial. Fig. 7A displays the relationship between the gut microbiota composition and SCFAs. It could be inferred that the abundance of Deferribacterota was significantly inversely associated with the levels of acetic acid, isobutyric acid, and isovaleric acid. Verrucomicrobiota, significantly modulated across different experimental groups, exhibited a significantly negative correlation with isobutyric acid, isovaleric acid, and butanoic acid. In contrast, acetic acid demonstrated a positive correlation with the abundance of Patescibacteria and Desulfobacteria.

Fig. 7B illustrats the associations between gut microbiota composition and neurotransmitter levels. In this study, Verrucomicrobiota, which was elevated in the APP/PS1 amnesia mouse model, exhibited a significant inverse correlation with 5-HT, Lys, DA, Spm, and Ser. Proteobacteria demonstrated a significant negative association with DA, Spm, Cys, and Gln. Conversely, Deferribacterota showed a notable correlation with Phe, Dopac, *L*-DOPA, and DA. Bacteroidota was significantly positively correlated with NE, while Campilobacterota was significantly positively associated with Spd and negatively with Phe. Patescibacteria presented a significant negative relationship with Glu and a positive one with Dopac. Desulfobacterota was significantly positively correlated with both Phe and Dopac. Lastly, Actinobacteriota was significantly negatively correlated with the levels of Kyn and Glu.

Fig. 7C shows that Campilobacterota had a significant positive correlation with AChR-α7 and AChE levels. Additionally, the neuroapoptotic ratio Bax/Bcl-2 was significantly positively correlated with the abundance of Verrucomicrobiota and Proteobacteria.

3.8 Identification of PS metabolic peptides in serum

Fig. S1 presents mass spectrometry data comparing peptide profiles in serum samples from mice receiving various treatments. Distinct peaks, each representing a unique peptide, demonstrate variable intensities indicative of differing peptide concentrations among the treatment groups. Notably, the intact PS and PAY sequences, identified in simulated digestion products from a prior study[9], were not detected in the serum samples. This absence might be attributable to the complex processes of digestion, absorption, and metabolic interactions within the organism, as well as potential crosslinking events. Additionally, the analytical method employed here, which was not a targeted approach typically facilitated by triple quadrupole mass spectrometry, might also account for this result. Fig. S2 reveals significant distinctions in the total ion chromatography (TIC) among the groups, with the PS+CA treatment group displaying the highest peptide intensities, corroborating the findings from Fig. S1. Of the more than 20 000 peptides identified across the treatments, 47 contained the PAY fragment. Remarkably, multiple peptides in the PS+CA group exhibited increased intensities compared to others, potentially linking these profiles to the group's observed neuroprotective effects.

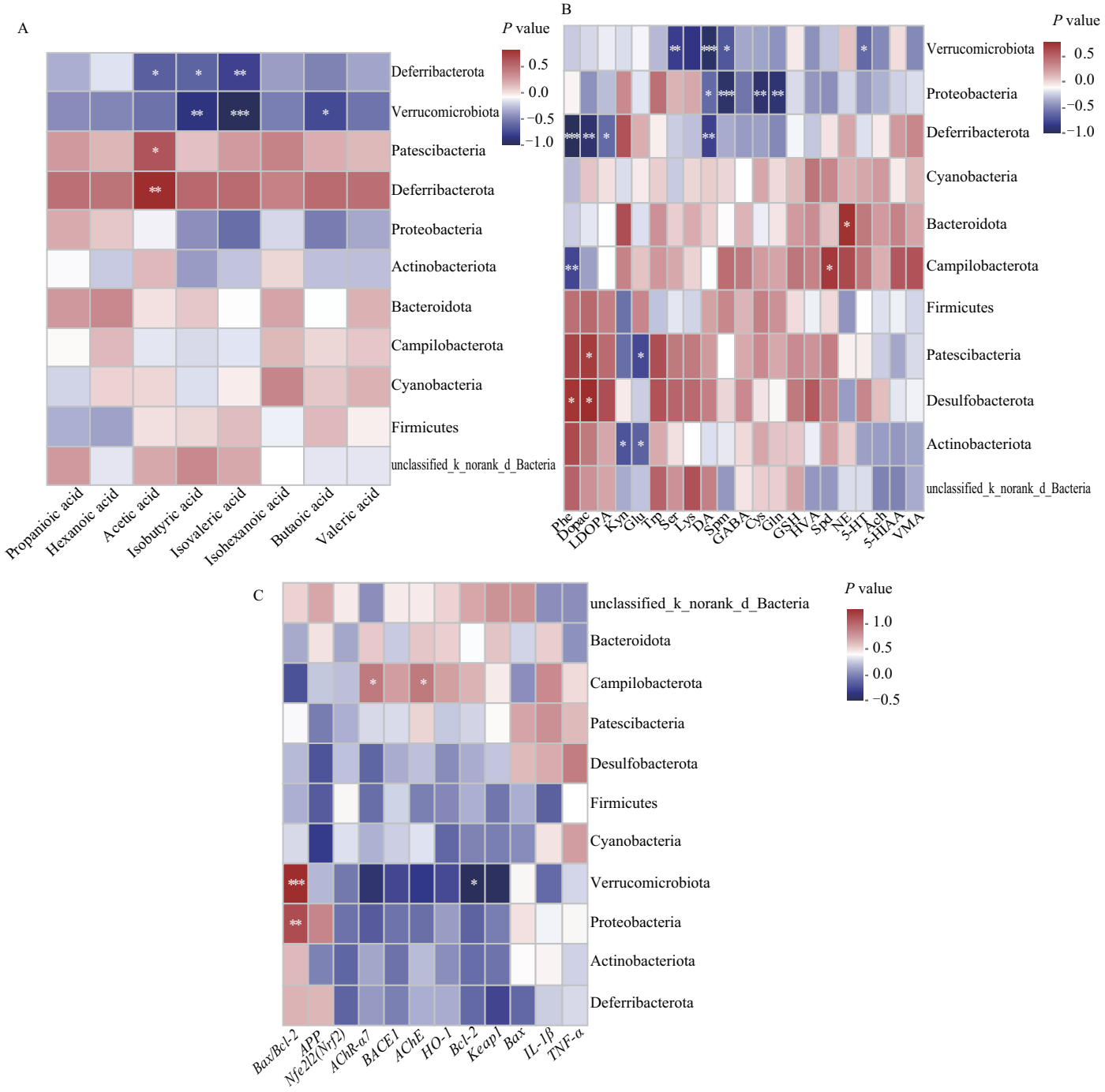

Fig. 7 Correlation analysis between gut microbiota and (A) SCFA, (B) brain neurotransmitters and (C) pathway factors. *$P < 0.05$, **$P < 0.01$, ***$P < 0.001$.

4. Discussion

AD, which is characterized by memory deficits, is associated with various mechanisms, including Aβ accumulation, oxidative stress, inflammatory responses, and neuro-related pathways. The administration of the neuroprotective peptide PS, derived from anchovy protein hydrolysates (APH), has been demonstrated to ameliorate memory deficits in scopolamine-induced amnesic mice[32]. However, its bioactivity may be compromised within the gastrointestinal system, which can hydrolyze PAYCS into PAY and additional peptide fragments[9]. Prior research has focused on enhancing the activity and stability of APH through interaction with CA[10,33]. Our previous work revealed that both covalent and non-covalent binding of PS and CA result in distinct bioactive effects. Yet, the comparative analysis of their functionalities, specifically in terms of memory improvement via non-covalent versus covalent interactions, remained unexplored. Therefore, this study was dedicated to the preparation and structural characterization of the covalent and non-covalent conjugates of PS and CA, with a subsequent evaluation of their efficacy in enhancing memory.

Chromatographic profiles depicted in Fig. 1 indicated that the PS-CA complex was characterized by a single chromatographic peak, suggesting a pure conjugate, while the PS+CA sample exhibited multiple peaks, indicative of a heterogeneous mixture. MS and MS/MS results revealed potential modifications to the Tyr and Cys residues in PS during the process of covalent conjugation. These alterations in molecular structure among PS-CA, PS+CA, and PS were likely to have significant implications for their biological activity. Huang et al.[34] examined the synergistic potential of peptide-polyphenol complexes, specifically KLVFF paired with EGCG, in attenuating Aβ aggregation and neurotoxicity. They discovered that the KLVFF/EGCG complex could enhance the inhibitory effect on $A\beta_{42}$ fibril formation more effectively than either KLVFF or EGCG alone. This enhanced inhibition was likely due to increased steric hindrance provided by the complex, which interferes with the extension of $A\beta_{42}$ fibrils.

In behavioral trials utilizing the APP/PS1 mouse model, differential therapeutic efficacy was observed, with various treatments mitigating memory impairment. This variance in efficacy may be ascribed to the unique modulatory effects of each compound on the gut-brain axis, underscoring a sophisticated interplay between molecular structure and physiological impact[35]. Converging lines of research consistently demonstrate a linkage between AD and gut microbiota dysbiosis[36-37], a finding corroborated in the APP/PS1 transgenic mouse model[38]. As depicted in Fig. 3, distinct microbial compositions and abundances were evident across various treatment groups. Notably, alterations in the abundance of Bacteroidota and Firmicutes were discernible (Fig. 3 and Table S2). Specifically, the Bacteroidota/Firmicutes (B/F) ratio was diminished in the APP/PS1 group (0.43) relative to the control (0.48). Post-treatment with PS-CA, PS+CA, and PS, the B/F ratios escalated to 1.82, 0.77, and 1.04, respectively. Similar modulations in Bacteroidota and Firmicutes abundance were also observed in APP/PS1 models exhibiting AD pathology[39]. Corresponding regulatory outcomes were reported by Tran et al.[40]. An insect extract was demonstrated to counteract the disruption of the blood-brain barrier and cerebral edema, alongside rectifying VPA-induced gut dysbiosis by restoring the B/F ratio in an autism model. Furthermore, an elevated abundance of Verrucomicrobiota has been reported in AD patients[41] and in models of sepsis-associated encephalopathy[42]. Our study identified a significantly higher prevalence of Verrucomicrobiota in the APP/PS1 model, which was substantially reduced following sample treatments. Liu et al.[42] established that probiotics (*Clostridium butyricum)* can influence neurodevelopment and cognitive functions by modulating the gut microbiota, particularly by diminishing Verrucomicrobiota abundance. Contrasting findings were presented by Li et al.[43], indicating that treatment with capsaicin resulted in a heightened abundance of Verrucomicrobiota compared to vehicle-treated APP/PS1 mice. Additionally, an upregulation of Verrucomicrobiota has been documented following dextran sodium sulfate induction in ulcerative colitis, potentially exacerbating gut permeability[44-45]. Notably, walnut-derived peptide PW5 was reported to be effective in modulating the abundance of Firmicutes and decreasing Verrucomicrobia in APP/PS1 transgenic mice[46].

SCFAs, like acetate (acetic acid), propionate (propanoic acid), and butyrate (butanoic acid), potentially offer neuroprotection linked to the gut microbiome. These SCFAs might also influence the development and activity of brain microglia, indicating their possible role in altering neuro-related pathways relevant to neurodegenerative diseases[38,47]. Especially, Butyrate and propionate can disrupt the oligomerization of $A\beta_{1-42}$ peptides[48]. Treatment combining PS+CA was shown to significantly increase levels of propionate and butyrate, while PS alone or PS-CA also increased propionate levels ($P < 0.05$, Fig. 4). Liu et al.[49] reported that sesamol reduced amyloid peptide buildup and cognitive decline in APP/PS1 mice by markedly raising SCFA concentrations, including acetate, propionate, isobutyrate, butyrate, and valerate. Furthermore, according to Fig. 7A, the concentrations of acetate, isobutyric acid, and butanoic acid were inversely correlated with the relative abundance of Verrucomicrobiota, which was elevated in APP/PS1 transgenic mice. Our results were in accordance with the study reported by Yang et al. that excessive abundance of Verrucomicrobiota might lead to a reduction in gastrointestinal SCFA concentrations[50]. This suggested a pivotal role for gut microbiota-SCFA-modulating treatments in mitigating memory deficits in mouse models of amnesia.

Alterations in gut microbiota and their metabolites could affect brain neurotransmitters[8]. Sample administration was shown to positively influence various neurotransmitter categories, including inhibitory (5-HT, DA, GABA), neuromodulatory (5-HT, Kyn, Trp), and excitatory (Glu, Ach, etc.) neurotransmitters, as well as polyamines. Notably, 5-HT, Trp, and Glu are crucial for memory processes[51-53]. Furthermore, polyamines such as Spd and Spm, essential for cell viability, proliferation, function, and differentiation, are inversely associated with brain aging[54]. In the APP/PS1 mouse model, Glu levels were elevated compared to the control group, and PS-CA treatment significantly reduced Glu levels in the brain. Maintaining a balance of Glu, the primary excitatory neurotransmitter in the mammalian central nervous system, is essential. Disruption of this balance may contribute to homeostatic loss in the APP/PS1 model. Merritt et al.[55] suggested that elevated Glu levels could act as a biomarker for the severity of schizophrenia. Collectively, these findings indicated that PS-CA, PS+CA, and PS might enhance memory by regulating neurotransmitter levels. As depicted in Fig. 7B, the abundance of Verrucomicrobiota negatively correlated with certain neurotransmitter levels, highlighting the significant impact of the samples on Verrucomicrobiota alterations.

The behavioral results related to memory loss in our study were linked to neuro-related pathways. Treatment with PS-CA, PS+CA, and PS notably modulated the expression of factors associated with the cholinergic system (AchE, AChR-α7) and neuroapoptosis (Bax and the bax/Bcl-2 ratio), although no significant effects were observed in the regulation of amyloid-beta accumulation (APP, BACE1), oxidative stress (Nrf2, Keap1), or inflammation (IL-1β, TNF-α) pathways. Notably, an upregulation of HO-1 was detected in the treatment groups. Cholinergic signaling, crucial for higher brain functions such as memory, learning, and attention[56], was modulated by these treatments. Our previous studies with a scopolamine-induced mouse model confirmed the neuroprotective effects of APH and PS through AChE inhibition and AChR regulation[32,57]. Within the Bcl-2 protein family, Bax (pro-apoptotic) and Bcl-2 (anti-apoptotic) function in opposition. Bcl-2 inhibits apoptosis, while Bax promotes Bcl-2 degradation, reducing its anti-apoptotic influence[58]. This study observed a significant down-regulation in the increased Bax/Bcl-2 ratio in APP/PS1 transgenic mice following treatment. These findings suggested that PS-CA and PS treatments enhance memory by regulating the cholinergic system and reversing neuronal apoptosis, while PS alone primarily inhibits neuronal apoptosis. Correlation analysis (Fig. 7) revealed a positive association between the cholinergic system and Campilobacterota abundance, and a significant positive correlation between neuronal apoptosis and the abundance of Verrucomicrobiota and Proteobacteria. These correlations aligned with the effects of PS-CA and PS+CA treatments on gut microbiota modifications. While not all oxidative stress-related factors were modulated, the treatment with PS-CA and PS+CA resulted in an upregulation of the antioxidant enzyme HO-1. Lee et al.[59] demonstrated that α-pinene increased the protein levels of antioxidant enzymes, particularly HO-1 and manganese superoxide dismutase, in the hippocampus of a scopolamine-induced AD mouse model. The changes of HO-1 might be also responsible for the content of GSH in the brain (Fig. 5).

The variations in bioactivities observed might arise from the structural alterations caused by the covalent and non-covalent modifications of PS by CA. Serum peptide identification results (Fig. S1) revealed that peptides derived from PAY were most prevalent in the PS+CA treated group. Additionally, the covalent bonding of CA with APH demonstrated synergistic memory enhancement in scopolamine-induced amnesic mice[10]. Consequently, the amnesia-alleviating effects of PS-CA and PS+CA exhibited distinct modulatory impacts on the gut-brain axis which was better than PS.

5. Conclusion

In this study, we prepared PS-CA and PS+CA products through alkali and physical treatments to produce covalent and non-covalent products, respectively. The PS-CA conjugate, featuring a newly formed compound with a Tyr-modified PS, was identified. Behavioral tests in APP/PS1 transgenic mice revealed that both covalent and non-covalent modifications of PS with CA enhanced memory, with PS-CA showing superior alleviation effects. 16S rRNA sequencing indicated alterations in specific microbiota abundances including the ratio of B/F under different treatments. Notably, Verrucomicrobiota abundance, significantly elevated in APP/PS1 mice, was substantially reduced by all treatments. Furthermore, neuroprotective SCFAs in the gut were positively influenced by the treatments, particularly PS+CA. Neurotransmitter analysis in the brain demonstrated a positive impact of these treatments, especially PS-CA, on neurotransmitter levels. The study identified key pathway factors, underscoring significant modulation of the cholinergic system, neuronal apoptosis, and antioxidant pathways by PS-CA and PS+CA. Correlation analysis suggested the regulatory effects of these treatments on Verrucomicrobiota as a key factor. Overall, this research highlights the memory-enhancing potential of the interaction between PS and CA in APP/PS1 transgenic mice through the gut-brain axis. Additionally, the differential targets of covalent and noncovalent conjugates should be subsequentially investigated. Furthermore, the specific structure of PS-CA, stability and bioavailability of PS-CA and PS+CA would be also explored. All these researches would provide a comprehensive understanding of different interaction ways on the structure, bioactivity and application between food-derived components.

Declaration of competing interest

The authors declare no competing financial interests.

Acknowledgements

This work was supported by the grants from the National Natural Science Foundation of China (32201980), Guangdong Provincial Natural Science Foundation General Project (2025A1515010320), Guangdong Academy of Agricultural Sciences Talent Development Young Researcher Program (R2023PY-QY011) and the Excellent Doctoral Talents Introduction Project of Guangdong Academy of Agricultural Sciences (R2021YJ-YB3006) and the Jinying Zhiguang Project of GDAAS (R2023PY-JG016).

Appendix A. Supplementary data

Supplementary data associated with this article can be found, in the online version, at http://doi.org/10.26599/FSHW.2024.9250402.

References

[1] FDA, Brochure: Maintaining Mental Function, 2022. https://www.fda.gov/consumers/minority-health-and-health-equity-resources/alzheimers-disease.

[2] T.G. Dinan, J.F. Cryan, The microbiome-gut-brain axis in health and disease, Gastroenterol. Clin. 46 (2017) 77-89. https://doi.org/10.1016/j.gtc.2016.09.007.

[3] V.V. Giridharan, C.E.B. De Quevedo, F. Petronilho, Microbiota-gut-brain axis in the Alzheimer's disease pathology-an overview, Neurosci. Res. 181 (2022) 17-21. https://doi.org/10.1016/j.neures.2022.05.003.

[4] S. Wu, Z.F. Bhat, R.S. Gounder, et al., Effect of dietary protein and processing on gut microbiota—a systematic review, Nutrients 14 (2022) 453. https://doi.org/10.3390/nu14030453.

[5] D. Serra, L.M. Almeida, T.C.P. Dinis, Dietary polyphenols: a novel strategy to modulate microbiota-gut-brain axis, Trends Food Sci. Technol. 78 (2018) 224-233. https://doi.org/10.1016/j.tifs.2018.06.007.

[6] S. Wu, A.E.D.A. Bekhit, Q. Wu, et al., Bioactive peptides and gut microbiota: candidates for a novel strategy for reduction and control of neurodegenerative diseases, Trends Food Sci. Technol. 108 (2021) 164-176. https://doi.org/10.1016/j.tifs.2020.12.019.

[7] M. Wang, W.K. Amakye, C. Gong, et al., Effect of oral and intraperitoneal administration of walnut-derived pentapeptide PW5 on cognitive impairments in $APP_{SWE}/PS1_{\Delta E9}$ mice, Free Radic. Biol. Med. 180 (2022) 191-197. https://doi.org/10.1016/j.freeradbiomed.2022.01.003.

[8] T. Zhao, S. Zhong, J. Xu, et al., PAYCS alleviates scopolamine-induced memory deficits in mice by reducing oxidative and inflammatory stress and modulation of gut microbiota-fecal metabolites-brain neurotransmitter axis, J. Agric. Food Chem. 70 (2022) 2864-2875. https://doi.org/10.1021/acs.jafc.1c06726.

[9] T. Zhao, L. Zheng, Q. Zhang, et al., Stability towards the gastrointestinal simulated digestion and bioactivity of PAYCS and its digestive product PAY with cognitive improving properties, Food Funct. 10 (2019) 2439-2449. https://doi.org/10.1039/c8fo02314j.

[10] T. Zhao, C. Zhang, S. Zhong, et al., Synergistic alleviation effects of anchovy hydrolysates-catechin on scopolamine-induced mice memory deficits: the exploration of the potential relationship among gut-brain-axis, Food Funct. 13 (2022) 1563-1578. https://doi.org/10.1039/D1FO02195H.

[11] X. Ni, C. Chen, R. Li, et al., Effects of ultrasonic treatment on the structure and functional characteristics of myofibrillar proteins from black soldier fly, Int. J. Biol. Macromol. 278 (2024) 135057. https://doi.org/10.1016/j.ijbiomac.2024.135057.

[12] R. Pérez-Gregorio, S. Soares, N. Mateus, et al., Bioactive peptides and dietary polyphenols: two sides of the same coin, Molecules 25 (2020) 3443. https://doi.org/10.3390/molecules25153443.

[13] Y. Meng, C. Li, Conformational changes and functional properties of whey protein isolate-polyphenol complexes formed by non-covalent interaction, Food Chem. 364 (2021) 129622. https://doi.org/10.1016/j.foodchem.2021.129622.

[14] N.E. Buitimea-Cantúa, J.A. Gutiérrez-Uribe, S.O. Serna-Saldívar, Phenolic-protein interactions: effects on food properties and health benefits, J. Med. Food. 21 (2018) 188-198. https://doi.org/10.1089/jmf.2017.0057.

[15] T. Wu, L. Lin, X. Zhang, et al., Covalent modification of soy protein hydrolysates by EGCG: improves the emulsifying and antioxidant properties, Food Res. Int. 164 (2023) 112317. https://doi.org/10.1016/j.foodres.2022.112317.

[16] W. Jia, D.S. Sethi, A.J. van der Goot, et al., Covalent and non-covalent modification of sunflower protein with chlorogenic acid: Identifying the critical ratios that affect techno-functionality, Food Hydrocoll. 131 (2022) 107800. https://doi.org/10.1016/j.foodhyd.2022.107800.

[17] K. Zhang, Q. Wen, T. Li, et al., Effect of covalent conjugation with chlorogenic acid and luteolin on allergenicity and functional properties of wheat gliadin, J. Cereal Sci. 106 (2022) 103484. https://doi.org/10.1016/j.jcs.2022.103484.

[18] J. Yi, Y. Fan, Y. Zhang, et al., Characterization of catechin-α-lactalbumin conjugates and the improvement in β-carotene retention in an oil-in-water nanoemulsion, Food Chem. 205 (2016) 73-80. https://doi.org/10.1016/j.foodchem.2016.03.005.

[19] I. Khalifa, J.M. Lorenzo, S.P. Bangar, et al., et al., Effect of the non-covalent and covalent interactions between proteins and mono- or di-glucoside anthocyanins on β-lactoglobulin-digestibility, Food Hydrocoll. 133 (2022) 107952. https://doi.org/10.1016/j.foodhyd.2022.107952.

[20] X. Li, M. Li, T. Zhang, et al., Enzymatic and nonenzymatic conjugates of lactoferrin and (−)-epigallocatechin gallate: formation, structure, functionality, and allergenicity, J. Agric. Food Chem. 69 (2021) 6291-6302. https://doi.org/10.1021/acs.jafc.1c01167.

[21] A.M. Hall, E.D. Roberson, Mouse models of Alzheimer's disease, Brain Res. Bull. 88 (2012) 3-12. https://doi.org/10.1016/j.brainresbull.2011.11.017.

[22] D. Mulder, E. Aarts, A. Arias Vasquez, et al., A systematic review exploring the association between the human gut microbiota and brain connectivity in health and disease, Mol. Psychiatry. (2023) 1-25. https://doi.org/10.1038/s41380-023-02146-4.

[23] Y.P. Silva, A. Bernardi, R.L. Frozza, The role of short-chain fatty acids from gut microbiota in gut-brain communication, Front. Endocrinol. 11 (2020) 25. https://doi.org/10.3389/fendo.2020.00025.

[24] L.M.T. Dicks, Gut bacteria and neurotransmitters, Microorganisms 10 (2022) 1-24. https://doi.org/10.3390/microorganisms10091838.

[25] C. Li, P. Long, M. He, et al., *Phyllanthus emblica* Linn. fruit polyphenols improve acute paradoxical sleep deprivation-induced cognitive impairment and anxiety *via* Nrf2 pathway, J. Funct. Foods 110 (2023) 105884. https://doi.org/10.1016/j.jff.2023.105884.

[26] K. Li, L. Yan, Y. Zhang, et al., Seahorse treatment improves depression-like behavior in mice exposed to CUMS through reducing inflammation/oxidants and restoring neurotransmitter and neurotrophin function, J. Ethnopharmacol. 250 (2020) 112487. https://doi.org/10.1016/j.jep.2019.112487.

[27] S. Wójtowicz, A.K. Strosznajder, M. Jeżyna, et al., The novel role of PPAR alpha in the brain: promising target in therapy of Alzheimer's disease and other neurodegenerative disorders, Neurochem. Res. 45 (2020) 972-988. https://doi.org/10.1007/s11064-020-02993-5.

[28] F. Trettel, M.A. Di Castro, C. Limatola, Chemokines: key molecules that orchestrate communication among neurons, microglia and astrocytes to preserve brain function, Neuroscience 439 (2020) 230-240. https://doi.org/10.1016/j.neuroscience.2019.07.035.

[29] M. Wu, T. Tian, Q. Mao, et al., Associations between disordered gut microbiota and changes of neurotransmitters and short-chain fatty acids in depressed mice, Transl. Psychiatry 10 (2020) 350. https://doi.org/10.1038/s41398-020-01038-3.

[30] B. Dalile, L. Van Oudenhove, B. Vervliet, et al., The role of short-chain fatty acids in microbiota-gut-brain communication, Nat. Rev. Gastroenterol. Hepatol. 16 (2019) 461-478. https://doi.org/10.1038/s41575-019-0157-3.

[31] X. Qian, X. Song, X. Liu, et al., Inflammatory pathways in Alzheimer's disease mediated by gut microbiota, Ageing Res. Rev. 68 (2021) 101317. https://doi.org/10.1016/j.arr.2021.101317.

[32] T. Zhao, G. Su, S. Wang, et al., Neuroprotective effects of acetylcholinesterase inhibitory peptides from anchovy (*Coilia mystus*) against glutamate-induced toxicity in PC12 cells, J. Agric. Food Chem. 65 (2017) 11192-11201. https://doi.org/10.1021/acs.jafc.7b03945.

[33] T. Zhao, L. Huang, D. Luo, et al., Fabrication and characterization of anchovy protein hydrolysates-polyphenol conjugates with stabilizing effects on fish oil emulsion, Food Chem. 351 (2021) 129324. https://doi.org/10.1016/j.foodchem.2021.129324.

[34] Q. Huang, Q. Zhao, J. Peng, et al., Peptide-polyphenol (KLVFF/EGCG) binary modulators for inhibiting aggregation and neurotoxicity of amyloid-β peptide, ACS Omega. 4 (2019) 4233-4242. https://doi.org/10.1021/acsomega.8b02797.

[35] L.H. Morais, H.L. Schreiber IV, S.K. Mazmanian, The gut microbiota-brain axis in behaviour and brain disorders, Nat. Rev. Microbiol. 19 (2021) 241-255. https://doi.org/10.1038/s41579-020-00460-0.

[36] Z.Q. Zhuang, L.L. Shen, W.W. Li, et al., Gut microbiota is altered in patients with Alzheimer's disease, J. Alzheimers Dis. Jad. 63 (2018) 1337-1346. https://doi.org/10.3233/JAD-180176.

[37] C.C. Hung, C.C. Chang, C.W. Huang, et al., Gut microbiota in patients with Alzheimer's disease spectrum: a systematic review and meta-analysis, Aging 14 (2022) 477. https://doi.org/10.18632/aging.203826.

[38] J. Sun, J. Xu, Y. Ling, et al., Fecal microbiota transplantation alleviated Alzheimer's disease-like pathogenesis in APP/PS1 transgenic mice, Transl. Psychiatry 9 (2019) 3. https://doi.org/10.1038/s41398-019-0525-3.

[39] M. Feng, T. Hou, M. Zhou, et al., Gut microbiota may be involved in Alzheimer's disease pathology by dysregulating pyrimidine metabolism in APP/PS1 mice, Front. Aging Neurosci. 14 (2022) 967747. https://doi.org/10.3389/fnagi.2022.967747.

[40] N.B. Tran, H. Lee, S.J. Lee, Extracts from the edible insects *Gryllus bimaculatus* and *Oxya chinensis* sinuosa as an effective postnatal therapy for improving autistic behavior through blood-brain barrier control and gut microbiota, J. Funct. Foods 104 (2023) 105516. https://doi.org/10.1016/j.jff.2023.105516.

[41] A. Kaiyrlykyzy, S. Kozhakhmetov, D. Babenko, et al., Study of gut microbiota alterations in Alzheimer's dementia patients from Kazakhstan, Sci. Rep. 12 (2022) 15115. https://doi.org/10.1038/s41598−022−19393−0.

[42] J. Liu, Y. Jin, H. Li, et al., Probiotics exert protective effect against sepsis-induced cognitive impairment by reversing gut microbiota abnormalities, J. Agric. Food Chem. 68 (2020) 14874-14883. https://doi.org/10.1021/acs.jafc.0c06332.

[43] J. Li, X. Liao, X. Yin, et al., Gut microbiome and serum metabolome profiles of capsaicin with cognitive benefits in APP/PS1 mice, Nutrients 15 (2022) 118. https://doi.org/10.3390/nu15010118.

[44] H. Lu, M. Shen, Y. Chen, et al., Alleviative effects of natural plant polysaccharides against DSS-induced ulcerative colitis *via* inhibiting inflammation and modulating gut microbiota, Food Res. Int. 167 (2023) 112630. https://doi.org/10.1016/j.foodres.2023.112630.

[45] F.S. Heravi, K. Naseri, H. Hu, Gut microbiota composition in patients with neurodegenerative disorders (Parkinson's and Alzheimer's) and healthy controls: a systematic review, Nutrients 15 (2023) 4365. https://doi.org/10.3390/nu15204365.

[46] M. Wang, W.K. Amakye, L. Guo, et al., Walnut-Derived peptide PW5 ameliorates cognitive impairments and alters gut microbiota in APP/PS1 transgenic mice, Mol. Nutr. Food Res. 63 (2019) 1-12. https://doi.org/10.1002/mnfr.201900326.

[47] K.J. O'Riordan, M.K. Collins, G.M. Moloney, et al., Short chain fatty acids: microbial metabolites for gut-brain axis signalling, Mol. Cell. Endocrinol. 546 (2022) 111572. https://doi.org/10.1016/j.mce.2022.111572.

[48] L. Ho, K. Ono, M. Tsuji, et al., Protective roles of intestinal microbiota derived short chain fatty acids in Alzheimer's disease-type beta-amyloid neuropathological mechanisms, Expert Rev. Neurother. 18 (2018) 83-90. https://doi.org/10.1080/14737175.2018.1400909.

[49] Q. Liu, T. Xie, Y. Xi, et al., Sesamol attenuates amyloid peptide accumulation and cognitive deficits in APP/PS1 mice: the mediating role of the gut-brain axis, J. Agric. Food Chem. 69 (2021) 12717−12729. https://doi.org/10.1021/acs.jafc.1c04687.

[50] Q. Yang, T. Li, S. Lyu, et al., Ovalbumin and its Maillard reaction products ameliorate dextran sulfate sodium-induced colitis by mitigating the imbalance of gut microbiota and metabolites, Int. J. Biol. Macromol. 222 (2022) 715-724. https://doi.org/10.1016/j.ijbiomac.2022.09.224.

[51] T. Sharp, N.M. Barnes, Central 5-HT receptors and their function: present and future, Neuropharmacology 177 (2020) 108155. https://doi.org/10.1016/j.neuropharm.2020.108155.

[52] K. Gao, C. Mu, A. Farzi, et al., Tryptophan metabolism: a link between the gut microbiota and brain, Adv. Nutr. 11 (2020) 709-723. https://doi.org/10.1093/advances/nmz127.

[53] C.H. Chang, C.H. Lin, H.Y. Lane, *D*-Glutamate and gut microbiota in Alzheimer's disease, Int. J. Mol. Sci. 21 (2020) 2676. https://doi.org/10.3390/ijms21082676.

[54] T.T. Xu, H. Li, Z. Dai, et al., Spermidine and spermine delay brain aging by inducing autophagy in SAMP8 mice, Aging 12 (2020) 6401. https://doi.10.18632/aging.103035.

[55] K. Merritt, P.K. McGuire, A. Egerton, et al., Association of age, antipsychotic medication, and symptom severity in schizophrenia with proton magnetic resonance spectroscopy brain glutamate level: a mega-analysis of individual participant-level data, JAMA Psychiatry 78 (2021) 667-681. https://doi.10.1001/jamapsychiatry.2021.0380.

[56] H. Hampel, M.M. Mesulam, A.C. Cuello, et al., The cholinergic system in the pathophysiology and treatment of Alzheimer's disease, Brain 141 (2018) 1917−1933. https://doi.org/10.1093/brain/awy132.

[57] T. Zhao, J. Xu, H. Zhao, et al., Antioxidant and anti-acetylcholinesterase activities of anchovy (*Coilia mystus*) protein hydrolysates and their memory-improving effects on scopolamine-induced amnesia mice, Int. J. Food Sci. Technol. 52 (2017) 504−510. https://doi.org/10.1111/ijfs.13306.

[58] A. Peña-Blanco, A.J. García-Sáez, Bax, Bak and beyond—mitochondrial performance in apoptosis, FEBS J. 285 (2018) 416-431. https://doi.org/10.1111/febs.14186.

[59] G.Y. Lee, C. Lee, G.H. Park, et al., Amelioration of scopolamine-induced learning and memory impairment by α-pinene in C57BL/6 mice, Mult. Bioactivities Tradit. Med. Herbs Treat. Neurodegener. Dis. 2017 (2017) 4926815. https://doi.org/10.1155/2017/4926815.